Cement & Concrete Composites 33 (2011) 763–770

Contents lists available at ScienceDirect

Cement & Concrete Composites

journal homepage: www.elsevier.com/locate/cemconcomp

Quantification of crack-healing in novel bacteria-based self-healing concrete

Virginie Wiktor *, Henk M. Jonkers

Delft University of Technology, Faculty of Civil Engineering & Geosciences, Section of Materials & Environment – Microlab, Stevinweg 1, 2628 CN Delft, The Netherlands

ARTICLE INFO

Article history:
Received 11 November 2010
Received in revised form 30 March 2011
Accepted 31 March 2011
Available online 7 April 2011

Keywords:
Self-healing
Cracks
Bacteria
Concrete

ABSTRACT

Crack formation is a commonly observed phenomenon in concrete structures. Although micro crack formation hardly affects structural properties of constructions, increased permeability due to micro crack networking may substantially reduce the durability of concrete structures due to risk of ingress of aggressive substances particularly in moist environments. In order to increase the often observed autogenous crack-healing potential of concrete, specific healing agents can be incorporated in the concrete matrix. The aim of this study was to quantify the crack-healing potential of a specific and novel two-component bio-chemical self-healing agent embedded in porous expanded clay particles, which act as reservoir particles and replace part of regular concrete aggregates. Upon crack formation the two-component bio-chemical agent consisting of bacterial spores and calcium lactate are released from the particle by crack ingress water. Subsequent bacterially mediated calcium carbonate formation results in physical closure of micro cracks. Experimental results showed crack-healing of up to 0.46 mm-wide cracks in bacterial concrete but only up to 0.18 mm-wide cracks in control specimens after 100 days submersion in water. That the observed doubling of crack-healing potential was indeed due to metabolic activity of bacteria was supported by oxygen profile measurements which revealed O_2 consumption by bacteria-based but not by control specimens. We therefore conclude that this novel bio-chemical self-healing agent shows potential for particularly increasing durability aspects of concrete constructions in wet environments.

1. Introduction

As it is strong, durable and relatively inexpensive, concrete is the most used construction material worldwide [1]. However, the presence of cracks may reduce the durability of concrete structures. Micro cracks are an almost unavoidable feature of ordinary concrete. If micro cracks form a continuous network they may substantially contribute to the permeability of the concrete, thereby reducing the concrete's resistance against ingress of aggressive substances [2]. Nevertheless, not all initial micro cracks develop into harmful or unstable cracks. A number of studies reported that under certain circumstances, small cracks in concrete can heal [2–11]. This phenomenon is known as 'autogenous healing' or 'self-healing' of concrete. The primary causes of autogenic healing are considered to be based on chemical, physical, and mechanical processes [2,4]. However, precipitation of calcium carbonate has been reported to be the most significant factor influencing the autogenous healing of concrete [4,7].

Besides autogenous healing, cracks may also be autonomously repaired by incorporating a specific healing agent within the matrix. Various healing agents have been proposed for enhancing the self-healing capacity of concrete. While most healing agents are chemically based [2,12–14], more recently the possible application of bacteria as self-healing agent has also been considered [1,15–18]. In a number of published studies the potential of calcite precipitating bacteria for concrete or limestone surface remediation or durability improvement was investigated [15,17,19–23]. The mechanism of bacterially mediated calcite precipitation in latter studies was primarily based on the enzymatic hydrolysis of urea. A potential drawback of this reaction mechanism is that for each carbonate ion two ammonium ions are simultaneously produced which may result in excessive environmental nitrogen loading [16]. Moreover, in these studies bacteria or derived ureolytic enzymes were externally applied on cracked concrete structures or test specimens. Thus the remediation mechanism in those studies cannot be defined as self-healing. Recently, Jonkers et al. [1,16,18] developed a two-component self-healing system that is composed of bacterial spores, which after germination catalyze the metabolic conversion of organic compounds (the second component) to calcium carbonate. Both components were mixed with the fresh cement paste, thus becoming an integral part of the concrete. They furthermore showed that incorporated bacteria and certain organic calcium salts such as calcium lactate functioning as calcium carbonate precursor did not negatively affect concrete compressive strength. However, the authors also observed that the functionality of bacterial mineral production of directly (unprotected) incorporated two-component healing agent was

* Corresponding author. Tel.: +31 (0)15 278 2731; fax: +31 (0)15 278 6383.
E-mail address: v.a.c.wiktor@tudelft.nl (V. Wiktor).

0958-9465/$ - see front matter © 2011 Elsevier Ltd. All rights reserved.
doi:10.1016/j.cemconcomp.2011.03.012

limited to young (1–7 days old) concrete specimens. It was hypothesized that the majority of incorporated bacterial spores apparently became crushed or inactivated by high alkalinity, resulting not only in loss of viability but also in decreased mineral-forming capacity in aged specimens.

In the present study protection by immobilization in porous expanded clay particles of the two-component bio-chemical healing agent prior to addition to the concrete mixture was tested as an alternative strategy to the direct mixing in order to substantially increase its service life functionality. In this manner, the expanded clay particles not only represent an internal reservoir but also constitute both a structural element of concrete as well as a protective matrix for the self-healing agent. Such a system should increase the viability and thus the time-related functionality of the bio-chemical self-healing agent. The main aim of this study was therefore to quantify the crack-healing ability of aged concrete specimens based on this two-component bio-chemical agent immobilized in expanded clay particles.

2. Materials and methods

2.1. Self-healing agent preparation

The bio-chemical two-component self-healing agent consisted of a mixture of calcium lactate and bacterial spores both embedded in expanded clay particles. Spores of a bacterial isolate obtained from alkaline lake soil (Wadi Natrun, Egypt) were used in this study. Sequence analysis of 16S rRNA gene of this bacterium revealed a 98.7% homology to *Bacillus alkalinitrilicus* an alkali-resistant soil bacterium [24]. Senescent cultures containing high number of spores were washed by repeated centrifugation and resuspension of the cell pellet in sterile tap water to harvest vegetative cells and spores. Suspensions were subsequently heated for 30 min at 80 °C to inactivate present vegetative cells and number of viable spores in suspensions were quantified by the most probable number cultivation–dilution technique. Light weight aggregates (LWA) (expanded clay particles Liapor R 1–4 mm, Liapor GmbH Germany) were impregnated twice under vacuum with a calcium lactate- (80 g/l), yeast extract- (1 g/l) solution, followed by a final impregnation step with a bacterial spore suspension. After each impregnation treatment, expanded clay particles were dried in an oven for 5 days at 37 °C. Obtained impregnated expanded clay particles contained 6% (by weight, in grams) calcium lactate and 1.7×10^5 bacterial spores g^{-1} particles.

2.2. Preparation of mortar test specimens

Reinforced mortar test specimens were prepared with ordinary Portland cement (CEMI 42.5N, ENCI, The Netherlands), fine aggregates (sand) and LWA either impregnated with bacterial spores and calcium lactate (bacteria-based specimens) or non-impregnated (control specimens). Table 1 shows applied mixing proportions.

Reinforced prismatic specimens with dimensions of $4 \times 4 \times 16$ cm were cast. In each specimen, one zinc plated steel bar (4 mm diameter, 26 cm long) was placed in the middle horizontal axis of the mold with both ends of the bar extending for 5 cm. After 24 h curing specimens were carefully unmolded, tightly sealed in plastic foil to avoid evaporation of water, and kept at room temperature for further curing.

After 56 days curing the specimen-embedded steel reinforcement bar was stretched by computer controlled application of tensile force resulting in the formation of multiple cracks, 12–14, in the mortar specimen. The widths of the induced cracks varied from 0.05 to 1 mm.

Table 1
Mixing proportion of mortar specimens.

Ingredients	Weight (g)
Cement	384
Water	192
Fine aggregates (0.125–1 mm)	929
LWA (1–4 mm)	292
W/C ratio	0.5

2.3. Self-healing incubation conditions

Two cracked mortar specimens (one control and one bacteria-based) featuring a high number of individual cracks with varying crack widths were immersed horizontally in tap water (3.5 cm water column covering the specimens) in a plastic bucket which was kept open to the atmosphere during the whole incubation period to allow free diffusion of oxygen and carbon dioxide over the water–air interface. Specimens were removed from water weekly for stereomicroscopic inspection and photographic imaging for quantification of crack-healing in time. Five cracks, with a total length of 53 mm, were monitored on each specimen.

Millimeter-sized extensive and partly crack-protruding precipitates, which only formed at crack surfaces of bacteria-based specimens, were manually removed for further analysis with the aid of pincers and a stereomicroscope. These precipitates were analyzed with an Environmental Scanning Electron Microscope (ESEM, Philips XL30 Series) equipped with an Energy Dispersive X-ray (EDAX) element analyzing system, and then examined by Fourier-Transform Infrared (FT-IR) spectrometry.

FT-IR spectra were collected on a Perkin–Elmer Spectrum 100 Series spectrometer equipped with universal Attenuated Total Reflexion (ATR) unit. The spectra were recorded in the range of 4000–650 cm^{-1} with 2 cm^{-1} resolution, and 32 scans were collected each time. The ATR analyses require very small amount of sample (<5 mg), and furthermore no preparation or dilution of the sample is needed. The FT-IR was first calibrated for background signal scanning, and then the experimental sample scanning was conducted.

The sampling operation simply consisted in removing the top part of the massive columnar precipitate formed at different locations of the cracks surface of bacteria-based specimen. Three different samples, named Bact a, Bact b and Bact c, were collected and investigated with ESEM and FT-IR.

Unlike bacteria-based mortar specimen, precipitates formed at cracks surfaces of control specimen were small and did not protrude from the crack surfaces. Latter aspect hampered collection of substantial amounts needed for respective analyses, which were therefore not possible on precipitates formed at crack surfaces of control specimens.

2.4. Oxygen consumption measurements

Oxygen is consumed by aerobic bacterial metabolic conversion of calcium lactate (Eq. (2)). We therefore used in this study optical oxygen microsensors (micro-optodes) for the quantification of oxygen consumption of water submersed control- and bio-chemical healing agent-containing mortar specimens. Oxygen uptake of a water submersed sample can be derived from a measured microprofile by calculating the change in oxygen concentration in the linear part of the gradient in the diffusive boundary layer using Fick's first law of diffusion (Eq. (1)) [25].

$$J = -D_{O_2} \frac{dC(z)}{dz} \quad (1)$$

where D_{O_2} is the diffusion coefficient of O_2 in water, and $C(z)$ is the concentration of O_2 at depth z.

The used oxygen microsensors type Oxy50M (Pyro-Science, Germany) feature a measuring range from 0 to 700 μM O_2. The actual sensing tip (∅ < 50 μm) is covered by a black coating to ensure that no measuring light from the optical oxygen detection escapes the sensor tip and furthermore to suppress any optical effects from the surrounding environment. The optical fiber is fixed in a syringe and guided through a hollow steel needle (40 mm long). For experimental measurements the oxygen microsensor was fixed to a motorized micromanipulator with a high-precision slide (0.1 μm resolution) for the vertical axis. Hence, automated and precise oxygen microprofile measurements were performed. Optical sensor readings were converted to oxygen concentrations by a Microx TX3-USB (Pyro-Science) optic oxygen meter. The oxygen microsensor is two-point calibrated: water–vapor saturated air (wet cotton wool in a vessel) and oxygen free solution (saturated Na_2SO_3 solution). Consult references [26,27] for further specific details concerning the fiber optic oxygen measurement technique.

Oxygen microprofiles were measured in vertical steps of 20 μm, from 5 mm above towards the surface of control- and bio-chemical agent-based mortar specimens in tap water at room temperature. The measurements are performed on fresh fractured samples of 9 months-old specimens cured in tap water. Each depicted profile represents the average of ten measurements performed at different locations. The calculated areal oxygen consumption rate based on the slope of the change in oxygen concentration through the linear part of the profile in the diffusive boundary layer (20.7 μM O_2 mm^{-1}) of the bio-chemical agent-based mortar specimen amounted to 4.14×10^{-2} μmol m^{-2} s^{-1}. In contrast, the oxygen consumption of the control specimen appeared insignificant.

3. Results

3.1. Optical determination of crack-healing capacity

Fig. 1 shows direct stereomicroscopic observation of cracks from control and bacteria-based specimens before and after 100 days of immersion in tap water. Width of completely healed cracks was significantly larger in bacteria-based specimens (0.46 mm) compared to control specimens (0.18 mm).

Element composition analysis using energy dispersive spectroscopy (EDAX) revealed that the massively formed precipitate on crack surfaces of bacterial specimens was essentially an association of calcium, oxygen and carbon atoms, what suggests that mineral precipitates were calcium carbonate ($CaCO_3$) based. The various crystal morphologies observed with environmental scanning electron microscopy (ESEM) differ however from the typical rhombohedral one of calcite (Fig. 2c–e). Two main morphologies were observed: "deformed" lamellar rhombohedra and needle-like clusters assembled in dumbbell shapes, possibly polymorphs of $CaCO_3$. As precipitation of substantial amounts of these apparent $CaCO_3$ polymorphs was only observed on crack surfaces of bacteria-based specimens it suggests that its formation was related to bacterial activity.

The Fourier-Transform InfraRed (FT-IR) spectra obtained from three different samples of this mineral precipitate are indicative of the presence of calcite and aragonite. The FT-IR spectra of $CaCO_3$ polymorphs have been extensively reported in the literature [28,29]. Because of their different crystal structure, they can be discriminated using FT-IR; a different spectrum is observed for each of the structural forms. Thus, the major vibrational bands for calcite are identified in the "Bact b" spectrum (Fig. 2f–h): C–O asymmetric stretching vibration (υ_3) of carbonates, C–O out of plan bending vibration (υ_2) of carbonates, C–O planar bending vibration (υ_4) of carbonates, centered at 1390, 871 and 712 cm^{-1} respectively. Spectral changes induced by the presence of aragonite are observed on the "Bact a" and "Bact c" spectra: broadening of the asymmetric bending vibration υ_3 (1500–1300 cm^{-1}) (Fig. 2f), the symmetric stretching vibration υ_1 becomes apparent (1040–1120 cm^{-1}) and the vibrations υ_2 (Fig. 2g) and υ_4 (Fig. 2h) are split. Unlike bacteria-based mortar specimen, precipitates formed at cracks surfaces of control specimen were small and did not protrude from the crack surfaces. Latter aspect hampered collection of substantial amounts

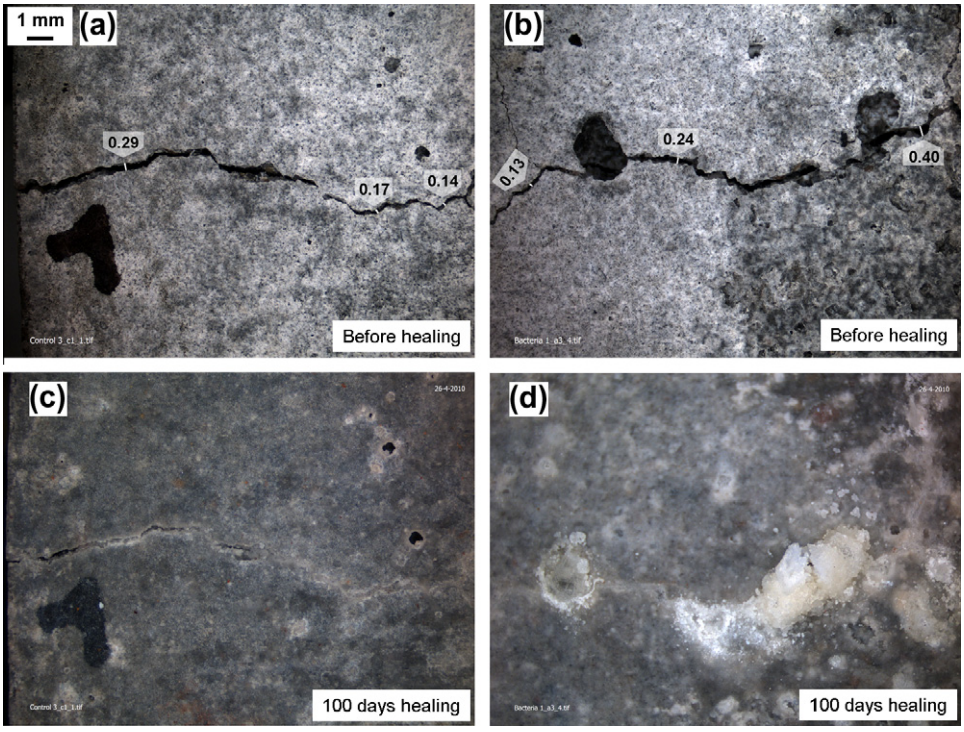

Fig. 1. Stereomicroscopic images of crack-healing process in control mortar specimen before (a) and after 100 days healing (c), in bio-chemical agent-based specimen before (b) and after 100 days healing (d).

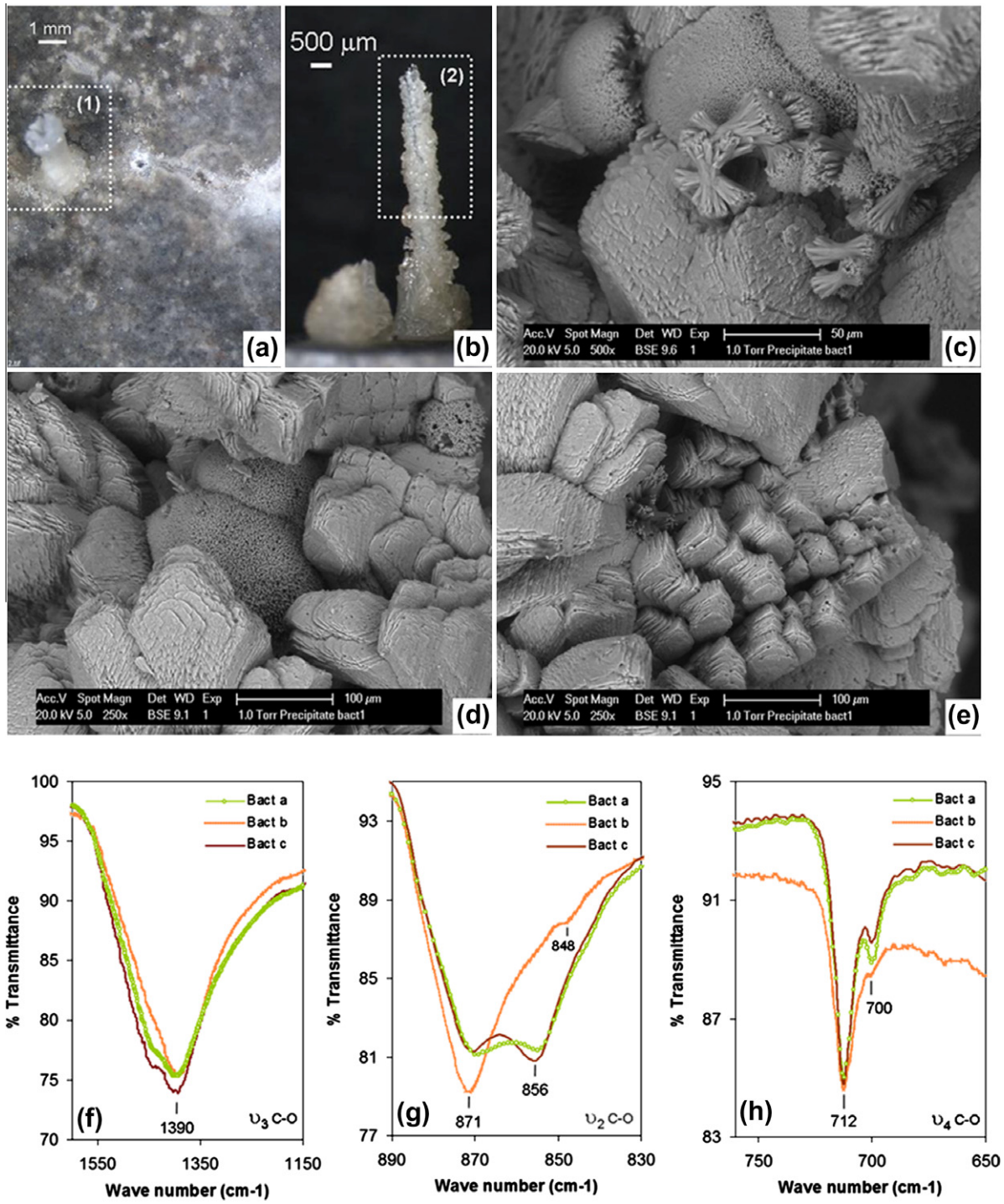

Fig. 2. Microscopic images of crack-filling precipitates after crack-healing (water submersion) of a bacteria-based specimen. (a) Stereomicroscopic overview image of crack with specific detail (massive columnar precipitate) indicated by dotted square, seen from above. (b) Stereomicroscopic close-up image of massive columnar precipitate (a1) seen from lateral side. (c–e) ESEM images of top part of massive columnar precipitate indicated in image (b2) by dotted square. (f) Details of the FT-IR spectra obtained from three different samples (a–c) of massive columnar precipitate observed on the cracks surface of bacteria-based specimen: C–O asymmetric stretching vibration (υ_3). (g) Details of the out of plan bending vibration υ_2 CO_3^{2-}. (h) Details of bands of the planar bending vibration υ_4 CO_3^{2-}.

needed for respective analyses, which were therefore not possible on precipitates formed at crack surfaces of control specimens.

3.2. Crack-healing quantification

While from a qualitative point of view, the higher healing capacity of bacteria-based mortar is obvious, the major aspect of this study is the actual quantification of this crack self-healing. Due to the used method of tensile deformation of test specimens, multiple cracks (12–14 cracks) on each specimen with various lengths and widths were generated. Cracks formed primarily perpendicularly or parallel to the embedded reinforcement axis. Within a single crack, however, its width varied substantially along its length. Therefore, for crack-healing quantification purposes, it

appeared not convenient to determine and compare changes in crack mean width. Instead, crack width was measured at regular intervals, every 0.4 mm along the length of each crack. Hence, every week crack width measurements were performed at the same locations and the healing (crack closure) percentage was calculated for each location according to

$$\text{healing } \% = \frac{Cw_i - Cw_t}{Cw_i} \times 100 \quad (2)$$

where Cw_i is the initial crack width, Cw_t the width measured at time t.

In total 150 measurements covering five distinct cracks in both control and bacteria-based mortar specimens were performed. Results are depicted in Fig. 3. The crack-healing quantification procedure confirmed the conclusion based on microscopic observation i.e. that after prolonged incubation, crack-healing was significantly higher in bacteria-based specimens. After 20 days incubation, the same tendency of crack-healing behavior was noticed for both control and bacteria-based specimens (Fig. 3a) as in both type of specimens a similar inverse relationship between crack width and healing percentage was found: the smaller the crack width, the higher the healing percentage observed. Moreover, it was found that only few locations were completely (100%) healed. However, with increasing incubation period, the crack-healing percentage of bacteria-based specimen significantly increased in comparison to control specimen. This is visualized in Fig. 3b–d where measurement data from control and bacteria-based specimens no longer form one homogeneous group as in Fig. 3a but separate in two different ones which become more distinct with increasing incubation time. After complete healing the corresponding measurement data are plotted as a 100% healing value. From the resulting plots the threshold of maximum crack width which can be healed can be derived. Here, the threshold value was determined as the crack width not completely healed in all replicate spots. These threshold values derived from the different incubation period plots clearly show that after 40 days the healing of the cracks is considerably enhanced in bacteria-based specimens compared to control specimens. Hence, after 100 days of immersion in tap water (Fig. 4a), in bacteria-based mortar specimens the maximum crack width which can be healed is more than twice the size (0.46 mm) of that in control specimens (0.18 mm).

3.3. Oxygen consumption of bacteria-based specimens

Oxygen concentration profile measurements towards the surface of submersed mortar specimens revealed that bacteria-based but not control specimens consumed O_2. Ten oxygen profiles were measured at different locations for both control and bacteria-based specimens. The depicted O_2 profiles shown in Fig. 4b are the mean value of the ten replicate profile measurements. The O_2 profile of the control specimens shows an almost homogenous and constant O_2 concentration in the 5-mm water column above the specimen surface. The minor decrease in O_2 concentration in the 0.2-mm water layer directly above the specimen surface is probably due to the oxidation of ferrous particles present in the light weight expanded clay particles embedded in the mortar specimens. In contrast, the O_2 concentration of the bacteria-based specimen progressively decreases in the diffusive boundary layer (the 0.5-mm water layer overlaying the specimen surface). The areal oxygen consumption rate of the bacteria-based specimen as calculated

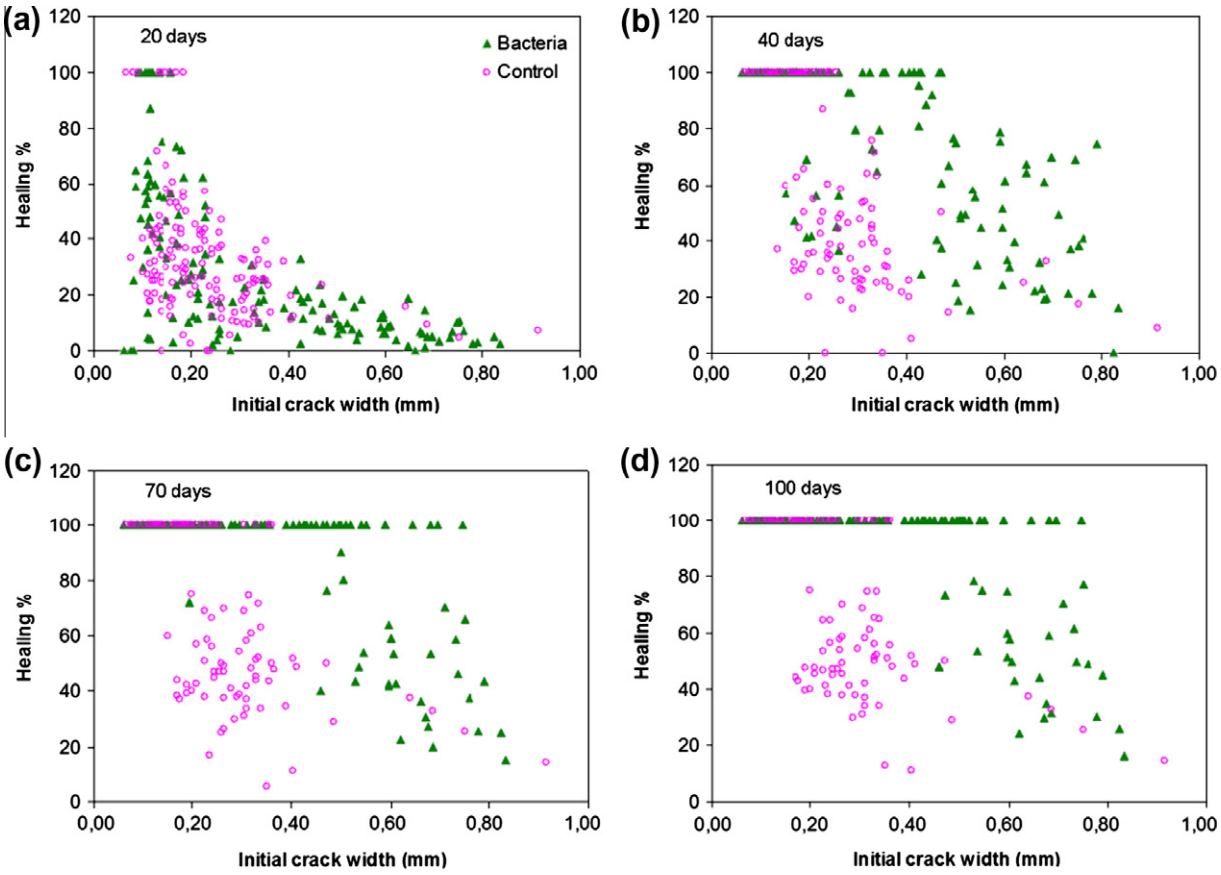

Fig. 3. Crack healing % as a function of the initial crack width for bio-chemical agent-based and control mortar specimens. For each, results from five cracks (150 measurements) are plotted after immersion time of (a) 20 days, (b) 40 days, (c) 70 days, and (d) 100 days.

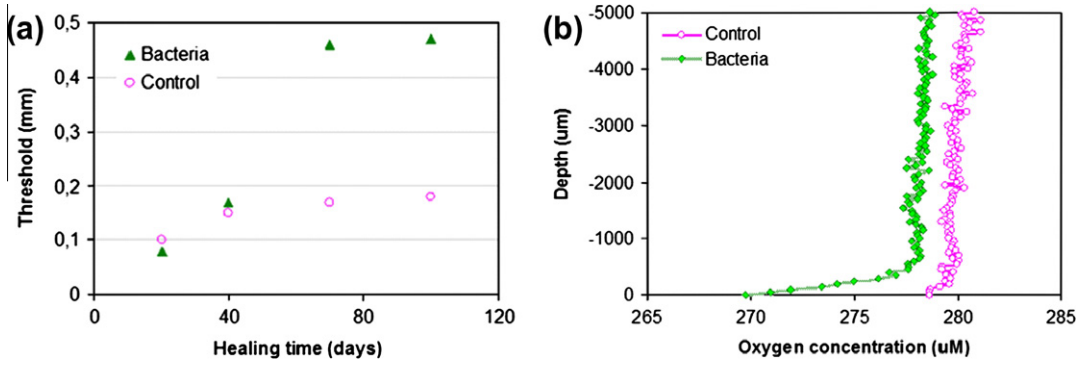

Fig. 4. (a) Threshold values of maximum crack widths healed after indicated healing time (submersion in water). (b) Measured oxygen concentration microprofiles towards surfaces of submerged control- and bio-chemical agent-based mortar specimens.

from the linear decrease in O_2 concentration in the diffusive boundary layer according to Fick's first law of diffusion equals 4.14×10^{-2} μmol m^{-2} s^{-1}.

4. Discussion

The self-healing is the partial or total recovery of at least one property of a material. In this study, the damage considered is the formation of cracks as it reduces the concrete's resistance against the ingress of aggressive substances; therefore the crack filling and/or closure is closely related to the recovery of the material permeability. Nevertheless, the sample geometry and size required to perform permeability test limit the number of cracks per sample, and the maximum crack width reachable. It was not possible to perform this test on our specimens, which were designed to obtain multiple and large cracks. Moreover, considering that the theoretical flow rate of a liquid through a cracked material is found to be proportional to the cube of the crack width, the permeability of a specimen with a larger crack will have a much greater permeability than a specimen with a smaller crack [30,31]. Although no direct permeability measurements were performed on the specimens investigated in this study, the monitoring of the crack closure over time gives a good indication about the improvement of the concrete permeability after the damage.

The objective of this study was to quantify the crack-healing capacity of concrete with embedded bio-chemical self-healing agent. The phenomenon of self-healing in concrete has been known for many years. It has been observed that some cracks in old concrete structures are lined with white crystalline material suggesting the ability of concrete to self-seal the cracks with chemical products by itself [14]. We also observed in the present study self-healing capacity of cracks in control specimens immersed in tap water. However, quantification of crack-healing revealed that autogenous healing in the control specimens was limited to crack widths up to 0.18 mm only. This is in good agreement with data reported in literature. The maximum crack width which can undergo autogenous healing was in several reported studies estimated to be between 0.1 and 0.3 mm, depending on exposure conditions [8,10,14,32–34]. The main processes involved in this abiotic autogenous healing were attributed to: (i) swelling and hydration of cement pastes, (ii) precipitation of calcium carbonates crystals, and (iii) blockage of flow paths due to deposition of water impurities or movement of concrete fragments that detach during the cracking process [2,4]. However, $CaCO_3$ precipitation seems to be the most significant factor influencing the autogenous healing [4,7]. The observation of white crystalline precipitate filling cracks of control specimens in the present study also suggests $CaCO_3$ formation, most probably due to natural carbonation of the cement paste.

In this study we additionally quantified crack-healing capacity of concrete featuring an inbuilt bio-chemical self-healing agent. The addition of the two-component self-healing agent, consisting of viable bacterial spores plus calcium lactate, significantly enhanced mineral precipitation on crack surfaces (Figs. 1d and 4a) resulting in healing of cracks with a maximal width of 0.46 mm, i.e. more than doubling the capacity of that of control specimens. The deposited minerals are likely calcium carbonate-based and form due to bacterial metabolic conversion of calcium lactate according to the reaction

$$CaC_6H_{10}O_6 + 6O_2 \rightarrow CaCO_3 + 5CO_2 + 5H_2O \quad (3)$$

The yield of $CaCO_3$ produced from calcium lactate will even increase when produced CO_2 molecules react with $Ca(OH)_2$ minerals (carbonation) which are quantitatively important hydration products of particularly Portland cement particles [16].

A further issue of this study was to find out whether the time dependent functionality of the two-component self-healing agent when immobilized in expanded clay particles prior to addition to the concrete mixture would increase in comparison to unprotected addition as was done in a previous study [16]. Results show indeed a major improvement as the functionality (mineral deposition on crack surfaces) increased from 7 days (previous study) to 100 days (present study). That increased mineral deposition in bacteria-based specimens is due to bacterial metabolic activity is supported by O_2 profile measurements in this study as these pointed out that O_2 consumption is, even several months after casting, substantial in bacteria-based specimens but only insignificant in control specimens (Fig. 4b). While in this study we focused on application of bacteria as inbuilt healing agent, in several previous studies the effect of external bacterially induced carbonate precipitation on building materials and in soils was investigated [15,19–23,35–38]. Several studies reported that the presence of bacteria affected the morphology and also the type of $CaCO_3$ precipitated [22,38,39]. In the present study the precipitates lining the crack surfaces of bacterial specimens and, which according to EDAX and FT-IR analysis appeared a mixture of calcite and aragonite, displayed primarily deformed rhombohedra and needle-like morphologies (Fig. 2c–e). These morphologies appear very similar to bacterially mediated types described in several reported studies. Lian et al. [38] noticed significant changes in shape and texture of calcite crystals formed in soils in presence of bacteria. The authors described the overall appearance of the crystals as resembling a three-dimensional cross. Such 3D crosses seemed to be formed as if the six faces on the rhombohedral nuclei began to extend solely in the direction normal to each surface. The additional formation of vaterite lead the authors conclude that the carbonate crystallization was strongly affected by bacteria. Rodriguez-Navarro et al. [22]

studying bacterial calcium carbonate production in porous ornamental limestone also noticed vaterite precipitation with typical morphologies of crystals (rhombohedra exhibiting preferred crystallographic orientation). Vaterite, the less stable $CaCO_3$ polymorph, and which can be chemically formed in highly calcium carbonate supersaturated solutions in laboratory, rapidly transforms into calcite or aragonite at room temperature in an aqueous solution [22,39]. It was therefore concluded that bacteria can enhance calcium carbonate precipitation through two mechanisms, i.e. providing as condensation nuclei a well-matched surface to seed $CaCO_3$ precipitation, as well as metabolically promoting calcium carbonate supersaturated conditions [22,38,39]. While aragonite usually displays an orthorhombic crystal structure and often appears as needles, vaterite instead commonly features spherulitic or disk-like precipitates [39]. As also supported by FT-IR investigations, we therefore assume that the observed needles-like morphologies and the rhombohedra-like deformed crystals in the present study are respectively aragonite- and calcite based.

5. Conclusion

In conclusion, the results presented in this study show that the applied two-component bio-chemical self-healing agent, consisting of a mixture of bacterial spores and calcium lactate, can be successfully applied to promote and enhance the self-healing capacity of concrete as the maximum healable crack width more than doubled. Moreover, oxygen measurements provided evidence that concrete incorporating bacterial spores embedded in expanded clay particles and derived active bacteria remain viable and functional several months after concrete casting.

The microbial enhanced crack-healing ability is presumably due to combined direct and indirect calcium carbonate formation: (i) direct $CaCO_3$ precipitation through metabolic conversion of calcium lactate (Eq. (2)) and (ii) indirect formation due to reaction of metabolically produced CO_2 molecules with $Ca(OH)_2$ minerals present in the concrete matrix leading to additional $CaCO_3$ precipitation.

In addition, as the metabolically active bacteria consume oxygen, the healing agent may act as an oxygen diffusion barrier protecting the steel reinforcement against corrosion. So far, bacteria have never been used to remove oxygen from the concrete matrix to inhibit reinforcement corrosion and further studies are needed to quantify this potentially additional beneficial process.

While in this study the enhanced self-healing capacity of bacteria-based concrete has been quantified, several other characteristics such as long-term (years) durability and cost efficiency of this novel type of concrete needs to be resolved before practical application can be considered. Anticipated potential advantages of this bacteria-based concrete are presumably primarily in reduction of maintenance and repair costs and extension of the service life of concrete constructions.

Acknowledgments

Arjan Thijssen and Ger Nagtegaal are acknowledged for help with ESEM analysis and laboratory support, Gerard Muyzer and Ben Abbas for 16S rRNA gene sequence analysis of the used bacterial isolate and Serge van Meer for help with FT-IR analysis. The authors acknowledge the financial support from Delft Centre for Materials (DCMat) in the form of Project SHM08704, 'Bio-chemical self-healing agent to prevent reinforcement corrosion in concrete'.

References

[1] Jonkers HM. Self-healing concrete: a biological approach. In: van der Zwaag S, editor. Self healing materials: an alternative approach to 20 centuries of materials science. The Netherlands: Springer; 2007. p. 195–204.
[2] Schlangen E, Joseph C. Self-healing processes in concrete. In: Gosh SK, editor. Self-healing materials: fundamentals, design strategies, and applications. Weinheim: Wiley-VCH verlag GmbH and Co KGaA; 2009. p. 141–82.
[3] Aldea CM, Song WJ, Popovics JS, Shah SP. Extent of healing of cracked normal strength concrete. J Mater Civil Eng 2000;12:92–6.
[4] Edvardsen C. Water permeability and autogenous healing of cracks in concrete. ACI Mater J 1999;96:448–54.
[5] Gerard B, Marchand J. Influence of cracking on the diffusion properties of cement-based materials – part I: influence of continuous cracks on the steady-state regime. Cem Concr Res 2000;30:37–43.
[6] Granger S, Loukili A, Pijaudier-Cabot G, Chanvillard G. Experimental characterization of the self-healing of cracks in an ultra high performance cementitious material: mechanical tests and acoustic emission analysis. Cem Concr Res 2007;37:519–27.
[7] Hearn N. Self-sealing, autogenous healing and continued hydration: what is the difference? Mater Struct 1998;31:563–7.
[8] Jacobsen S, Marchand J, Boisvert L. Effect of cracking and healing on chloride transport in OPC concrete. Cem Concr Res 1996;26:869–81.
[9] Parks J, Edwards M, Vikesland P, Dudi A. Effects of bulk water chemistry on autogenous healing of concrete. J Mater Civil Eng 2010;22:515–24.
[10] Reinhardt HW, Jooss M. Permeability and self-healing of cracked concrete as a function of temperature and crack width. Cem Concr Res 2003;33:981–5.
[11] Zhong WH, Yao W. Influence of damage degree on self-healing of concrete. Constr Build Mater 2008;22:1137–42.
[12] Dry CM. Three designs for the internal release of sealants, adhesives, and waterproofing chemicals into concrete to reduce permeability. Cem Concr Res 2000;30:1969–77.
[13] Joseph C. Experimental and numerical study of the fracture and self-healing of cementitious materials. PhD thesis, Cardiff, Cardiff University; 2008.
[14] Li VC, Yang EH. Self-healing in concrete materials. In: van der Zwaag S, editor. Self healing materials: an alternative approach to 20 centuries of materials science. The Netherlands: Springer; 2007. p. 161–93.
[15] De Muynck W, De Belie N, Verstraete W. Microbial carbonate precipitation improves the durability of cementitious materials: a review. Ecol Eng 2010;36:118–36.
[16] Jonkers HM, Thijssen A, Muyzer G, Copuroglu O, Schlangen E. Application of bacteria as self-healing agent for the development of sustainable concrete. Ecol Eng 2010;36:230–5.
[17] Ramachandran SK, Ramakrishnan V, Bang SS. Remediation of concrete using micro-organisms. ACI Mater J 2001;98:3–9.
[18] Jonkers HM, Schlangen E. A two component bacteria-based self-healing concrete. In: Alexander MG, Beushausen HD, Dehn F, Moyo P, editors. Concrete repair, rehabilitation and retrofitting II. Boca Raton: CRC Press, Taylor and Francis Group; 2009. p. 119–20.
[19] Bang SS, Galinat JK, Ramakrishnan V. Calcite precipitation induced by polyurethane-immobilized *Bacillus pasteurii*. Enzyme Microb Technol 2001;28:404–9.
[20] De Muynck W, Debrouwer D, De Belie N, Verstraete W. Bacterial carbonate precipitation improves the durability of cementitious materials. Cem Concr Res 2008;38:1005–14.
[21] Dick J, De Windt W, De Graef B, Saveyn H, Van der Meeren P, et al. Bio-deposition of a calcium carbonate layer on degraded limestone by *Bacillus* species. Biodegradation 2006;17:357–67.
[22] Rodriguez-Navarro C, Rodriguez-Gallego M, Ben Chekroun K, Gonzalez-Munoz MT. Conservation of ornamental stone by *Myxococcus xanthus*-induced carbonate biomineralization. Appl Environ Microbiol 2003;69:2182–93.
[23] van Tittelboom K, De Belie N, De Muynck W, Verstraete W. Use of bacteria to repair cracks in concrete. Cem Concr Res 2010;40:157–66.
[24] Sorokin DY, van Pelt S, Tourova TP. Utilization of aliphatic nitriles under haloalkaline conditions by *Bacillus alkalinitrilicus* sp. nov isolated from soda solonchak soil. FEMS Microbiol Lett 2008;288:235–40.
[25] Gundersen JK, Jorgensen BB. Microstructure of diffusive boundary-layers and the oxygen-uptake of the sea-floor. Nature 1990;345:604–7.
[26] Mock T, Dieckmann GS, Haas C, Krell A, Tison JL, et al. Micro-optodes in sea ice: a new approach to investigate oxygen dynamics during sea ice formation. Aquat Microb Ecol 2002;29:297–306.
[27] Presens. Instruction manual MICROX TX3: fiber optic meter, software version TX3v531. Presens – precision sensing GmbH; 2006.
[28] Gadsden JA. Infrared spectra of minerals and related inorganic compounds. London: Butterworths; 1975.
[29] Ghosh SN. IR spectroscopy. In: Ramachandran VS, Beaudoin JJ, editors. Handbook of analytical techniques in concrete science and technology. Principles, techniques, and applications. New-York: Noyes Publications, William Andrew Publishing; 2001. p. 174–204.
[30] Rapoport J, Aldea CM, Shah SP, Ankenman B, Karr AF. Permeability of cracked steel fiber-reinforced concrete. J Mater Civil Eng 2002;14(4):355–8.
[31] Hoseini M, Bindiganavile V, Banthia N. The effect of mechanical stress on permeability of concrete: a review. Cem Concr Compos 2009;31:213–20.
[32] Neville A. Properties of concrete. Harlow: Pearson Prentice Hall; 1995.
[33] ter Heid N, Schlangen E, van Breugel K. Experimental study of crack healing of early age cracks. In: Proceedings Knud Hojgaard conference on advanced cement-based materials, Lyngby, Denmark; 2005. p. 155–66.
[34] Qian SZ, Zhou J, Schlangen E. Influence of curing condition and precracking time on the self-healing behavior of engineered cementitious composites. Cem Concr Compos 2010;32:686–93.

[35] Castanier S, Le Metayer-Levrel G, Perthuisot JP. Ca–carbonates precipitation and limestone genesis – the microbiologist point of view. Sediment Geol 1999;126:9–23.
[36] De Muynck W, Verbeken K, De Belie N, Verstraete W. Influence of urea and calcium dosage on the effectiveness of bacterially induced carbonate precipitation on limestone. Ecol Eng 2010;36:99–111.
[37] Morita RY. Calcite precipitation by marine-bacteria. Geomicrobiol J 1980;2:63–82.
[38] Lian B, Hu QN, Chen J, Ji JF, Teng HH. Carbonate biomineralization induced by soil bacterium *Bacillus megaterium*. Geochim Cosmochim Acta 2006;70:5522–35.
[39] Warren LA, Maurice PA, Parmar N, Ferris FG. Microbially mediated calcium carbonate precipitation: implications for interpreting calcite precipitation and for solid-phase capture of inorganic contaminants. Geomicrobiol J 2001;18:93–115.